ELSEVIER

www.elsevier.nl/locate/carres

Carbohydrate Research 328 (2000) 549–559

CARBOHYDRATE RESEARCH

CP-MAS NMR analysis of carbohydrate fractions of soybean hulls and endosperm

Carel T.M. Fransen [a], Harmen van Laar [b], Johannis P. Kamerling [a], Johannes F.G. Vliegenthart [a,*]

[a] *Department of Bio-Organic Chemistry, Bijvoet Center, Utrecht University, PO Box 80075, NL-3508 TB Utrecht, The Netherlands*

[b] *Department of Animal Sciences, Animal Nutrition Group, Wageningen Institute of Animal Sciences (WIAS), Wageningen Agricultural University, PO Box 338, NL-6700 AH Wageningen, The Netherlands*

Received 26 October 1999; received in revised form 18 April 2000; accepted 18 April 2000

Abstract

CP-MAS NMR spectroscopy was used to identify soybean cellulose and pectin extracts and to investigate the kinetics of cross polarization. The in vitro incubation of cellulose and pectin, extracted from soya hull and endosperm, respectively, with sheep rumen fluid was followed with this technique. The difference in enzymatic degradability between ChSS and DASS, two pectins with identical monosaccharide composition, was explained by the degree of esterification that is lower in DASS. Variable contact time CP-MAS NMR experiments of the cellulose fraction during the incubation revealed that cellulose was degraded in a layer-by-layer way.

Keywords: Soybean; Cellulose; Pectin; CP-MAS NMR

1. Introduction

Soybean meal, the product obtained after extraction of oil from the beans, is used as animal feed. It is composed mainly of proteins and such polysaccharides as cellulose, starch, and pectins. Detailed knowledge about the molecular structure of these carbohydrates can help to develop approaches to improve the microbial degradation of these materials in ruminants and monogastrics. Furthermore, these polysaccharides constitute the most important structures found in plant cell walls. Consequently, new information may be used to enhance the food value of similar materials or for structure–function studies of plant polysaccharides. Thus far, various factors influencing microbial degradation have been determined, such as the polysaccharides present, their composition, and crystallinity [1], degree of esterification, acetylation [2], and cross linking.

Some decades ago, soybean polysaccharides were investigated by Morita et al. [3–5], Aspinall et al. [6–11] and Labavitch et al. [12]. Arabinogalactans and pectin-like polymers were proposed to occur in sodium hydroxide extracts. Because neutral carbohydrate side-chains might have been removed under those conditions [13,14], a new study towards soy-

* Corresponding author. Tel.: +31-30-2532184; fax: +31-30-2540980.

E-mail address: vlieg@accu.uu.nl (J.F.G. Vliegenthart).

0008-6215/00/$ - see front matter
PII: S0008-6215(00)00138-5

bean meal polysaccharides was started, using a mild extraction procedure with 1,2-diaminocyclohexane–*N*,*N*,*N*′,*N*′-tetraacetic acid (CDTA) yielding a chelating agent soluble solids (ChSS) fraction, which is a pectin [15]. Treatment of ChSS with arabinase, arabinofuranosidase B, and endo- and exo-galactanase yielded a smaller polymer, P. Structural analysis of ChSS, P, and mild acid hydrolysates of P indicated the presence of xylogalacturonan and rhamnogalacturonan, with arabinogalactan side chains in ChSS [16,17]. Unfortunately, solution-state NMR spectroscopy could not give any detailed structural information on ChSS and P because of the broad lines of the different signals. Therefore, we decided to use solid state NMR spectroscopy to study ChSS and water unextractable solids (WUS = carbohydrate fraction before CDTA extraction) from soybean hulls (SHW) and endosperm (SEW).

SHW and SEW were subjected to fermentation by rumen fluid of sheep. During the incubations, the dry weight and the monosaccharide composition of the residue were determined [18]. These samples were subjected to CP-MAS NMR analysis in order to study the applicability of this technique for obtaining additional information about the material. Variable contact-time CP-MAS NMR experiments were applied to obtain structural and motional information, and to investigate the kinetics of cross polarization [19–22] of the constituting polysaccharides. In these experiments, the signal intensity depends on the contact time (t) allowed for cross polarization. The relation between the signal intensity and the contact time can be fitted to an exponential curve with time constants T_{CH} and $T_{1\rho}$, used to describe the rising and falling part of the curve, respectively [20,21]. T_{CH} is a time constant defining the transfer rate of proton to carbon magnetization during the cross polarization contact, and $T_{1\rho}$ is the proton spin-lattice relaxation time in the rotating frame. A general rule that holds for large polymers [19,23] is that the lower the $T_{1\rho}$ value, the more mobile the polymer.

2. Theory

Variable contact-time experiments.—The correlation between ^{13}C signal intensity and the cross polarization time (t) can be described with a mono-phase model containing two exponential functions to account for the rising and falling part of the signal intensity curve as a function of the contact time. Mono-phase analysis was based on the equation:

$$M = M_0 \frac{\exp(-t/T_{1\rho}) - \exp(-t/T_{CH})}{1 - T_{CH}/T_{1\rho}} \quad (1)$$

where M = signal intensity, M_0 = calculated maximum signal intensity, t = contact time, $T_{1\rho}$ = proton spin lattice relaxation time in the rotating frame, and T_{CH} = time constant for cross polarization exponential buildup [20,21].

Alternatively, the relation between the signal intensity and the contact time can be described with two exponential functions for the rising and two for the falling part of the signal intensity curve. This two-phase analysis was based on the equation:

$$M = M_{0\,A} \frac{\exp(-t/T_{1\rho\,A}) - \exp(-t/T_{CH\,A})}{1 - T_{CH\,A}/T_{1\rho\,A}} + M_{0\,B} \frac{\exp(-t/T_{1\rho\,B}) - \exp(-t/T_{CH\,B})}{1 - T_{CH\,B}/T_{1\rho\,B}} \quad (2)$$

where the additional suffixes A and B refer to phases A and B, respectively. Two-phase analysis can be used to describe the magnetization as a sum of fast and slow polarization transfer. The fast process originates from protons attached to a carbon atom, whereas the slow one emanates from the non-bonded proton pool. The ratio between $M_{0\,A}$ and $M_{0\,B}$ (A/B in Tables 1–3, 5 and 6) indicates the relative amount of each phase in the description of the magnetization. Generally, two-phase analyses give a better fitting of the experimental results [24]. Contrary to Ref. [24], we used separate $T_{1\rho}$ values for the two phases. When no protons are bound to carbonyl carbons, the relationship between the signal intensity of these atoms and the contact time is described with the mono-phase model.

3. Results and discussion

Characterization and the fermentation of SHW.—The in vitro fermentation of SHW with rumen fluid of sheep fed medium-quality hay was monitored by measuring the cumulative gas production [25] and the monosaccharide composition [18], and by recording CP-MAS spectra of the material after 0, 12, 24, 36, and 48 h of incubation, respectively. The assignment of the signals in the CP-MAS spectra of SHW0 (SHW with 0 h of incubation with the sheep rumen fluid) and SHW48 are indicated in Tables 1 and 2, respectively. The CP-MAS spectrum of SHW0 (Fig. 1(A)) reveals that cellulose is the main component in this sample. This is in agreement with the monosaccharide analysis, showing 75% (w/w) of the total amount of carbohydrate to be glucose. During the incubation of SHW with sheep rumen fluid, cellulose is degraded as is shown by the decreasing signal-to-noise ratio of the cellulose signals in the spectra of SHW12-48 (Fig. 1(B–E)). Furthermore, new

Table 1
Resonance assignments and fitting parameters [a] for the variable contact time experiment on SHW0 [b]

Signal	Assignment [c]	$T_{CH\,A}$	$T_{1\rho\,A}$	$T_{CH\,B}$	$T_{1\rho\,B}$	A/B
105.5	cellulose C-1	0.37	11.7	0.01	0.4	2.7
102.5–95	pectic and other C-1	0.46	5.1	0.02	5.1	0.9
89	cellulose C-4 crystal interiors	0.41	12.5	0.02	12.5	1.4
87.2–83.3	cellulose C-4 crystal surfaces and non-crystalline cellulose	0.35	9.0	0.01	11.5	1.4
83.3–80.0	cellulose C-4 crystal surfaces and non-crystalline cellulose	0.47	12.7	0.03	4.5	1.0
75.5	cellulose C-2,3,5	0.37	13.5	0.02	7.1	1.5
72.5	cellulose C-2,3,5	0.40	12.9	0.01	10.2	1.4
65.5	cellulose C-6 crystalline cellulose	0.37	15.4	0.01	9.6	0.7
64–58.3	cellulose C-6 non-crystalline cellulose	0.40	10.2	0.01	0.5	1.7

[a] The evaluation of the variable contact time experiments is based on the two-phase model (Eq. (2)), except for carbonyl functions, which were evaluated with the mono-phase model (Eq. (1)). A/B represents the ratio between phase A and B.
[b] All time constants are in ms.
[c] Assignments based on data in Refs. [22,34].

Table 2
Resonance assignments and fitting parameters [a] for the variable contact time experiment on SHW48 [b]

Signal	Assignment [c]	$T_{CH\,A}$	$T_{1\rho\,A}$	$T_{CH\,B}$	$T_{1\rho\,B}$	A/B
187.3–168.3	C=O (carboxyl)	0.44	16.0			
135.7–125.7	aromatic C	0.29	8.8	0.03	9.9	1.13
110.8–99.2	C-1 (cellulose)	0.45	12.0	0.04	12.0	0.82
92.2–86.2	cellulose C-4 + degr. prod.	0.44	14.1	0.04	14.0	0.66
86.2–80.9	cellulose C-4 + degr. prod.	0.23	9.9	0.01	9.9	1.86
80.9–77.3	cellulose C-4 + degr. prod.	0.25	10.3	0.01	8.5	1.21
77.3–74	cellulose C-2,3,5	0.26	12.6	0.01	12.5	1.44
74–70	cellulose C-2,3,5	0.32	12.7	0.02	12.7	1.13
70–67.2	degr. prod.	0.17	9.8	0.01	4.2	1.43
67.2–64.2	C-6	0.29	16.0	0.01	8.7	0.71
64.2–59	cellulose C-6 non-crystalline cellulose	0.20	11.9	0.01	6.3	0.93
59–46.1	degr. prod.	0.30	9.1	0.01	5.1	1.11
46.1–36.8	degr. prod.	0.31	9.1	< 0.01	4.5	0.69
36.8–32	degr. prod.	0.21	13.7	0.01	4.5	1.23
32–10.1	degr. prod.	0.26	13.7	0.03	4.2	1.68

[a] The evaluation of the variable contact time experiments is based on the two-phase model (Eq. (2)), except for carbonyl functions, which were evaluated with the mono-phase model (Eq. (1)). A/B represents the ratio between phase A and B.
[b] All time constants are in ms.
[c] Assignments based on data in Refs. [22,34]; degr. prod. = degradation product.

Table 3
Resonance assignments and fitting parameters [a] for the variable contact time experiment on SEW [b]

Signal	Assignment [c]	$T_{CH\,A}$	$T_{1\rho\,A}$	$T_{CH\,B}$	$T_{1\rho\,B}$	A/B
182–170	C=O (carboxyl)	1.11	12.8			
113–107.5	C-1	0.19	3.8	0.01	1.3	3.8
107.5–103.2	C-1	0.29	6.0	0.01	3.3	2.0
103.2–96.7	C-1	0.49	3.4	0.07	3.6	0.7
91–83.5	C-5 GalA, subst. ring carbon	0.64	5.0	0.06	2.1	1.0
83.5–78.4	substituted ring carbon	0.33	4.0	0.01	4.0	1.6
78.4–67.2	C-2,3,4,5	0.32	5.3	<0.01	4.5	1.6
67.2–63.9	C-6	0.88	6.8	0.05	2.6	0.6
63.9–56.2	C-6	0.12	3.6	0.02	3.1	2.0
56.2–50.7	Me-ester	5.99	<0.1	0.53	3.1	0.2
36–10	Rha C-6, acetyl CH_3	1.33	1.2			

[a] The evaluation of the variable contact time experiments is based on the two-phase model (Eq. (2)), except for Rha C-6, acetyl CH_3 (due to the low signal intensity) and carbonyl functions, which were evaluated with the mono-phase model (Eq. (1)). A/B represents the ratio between phase A and B.
[b] All time constants are in ms.
[c] Assignments of the different pectic signals are based on data in Ref. [17].

signals appear in the CP-MAS spectra (δ 180–170, 132–126, and 45–10). These were assigned to degradation products and microbes grown during the fermentation experiment.

Characterization and the fermentation of SEW.—The in vitro fermentation of SEW was performed and monitored as described for SHW. CP-MAS spectra of SEW during the incubation are shown in Fig. 2. Tentative assignments of the signals in the CP-MAS spectra are given in Table 3. During the first 12 h of incubation, the relative ratio between the different monosaccharides remained constant. Furthermore, the total amount of carbohydrate decreased only slightly from 65 to 62.7% (w/w), as shown by monosaccharide analysis [18]. This is in agreement with the NMR spectra of SEW0 and SEW12, being almost identical.

After 24 h of incubation, the relative amount of galactose and arabinose decreased significantly (from 21.8 to 3.2% (w/w) and from 11.1 to 5.1% (w/w), respectively). These results suggest that pectic arabinogalactan side chains are degraded in this period. Some differences can be observed in the CP-MAS spectrum of SEW24 (Fig. 2(C)) in comparison with the starting material. The increase in the signals stemming from microbes and degradation products (δ 180–170 and 35–10, see SHW48) is most striking. Furthermore, the sharp signal in the anomeric region (δ 106) and the left part of the sharp signal at δ 74 have disappeared. From these results it was concluded that the signals that disappeared in the CP-MAS spectrum belonged to the arabinogalactan side chains of the polymer. Since these signals are relatively sharp, these side chains are expected to be more mobile than the rest of the polymer. This is in agreement with the result of an enzymatic degradation study, and solution state NMR analysis of ChSS and P [16,17]. The NMR study showed broad and sharp signals in the spectrum of ChSS, and only broad lines in the spectrum of P, which was explained by the absence of the arabinogalactan side chains in P.

In the subsequent course of the incubation (36 and 48 h) carbohydrate degradation continues. This could be concluded from the total amount of carbohydrate, being 20.1% (w/w) in SEW36 and 5.9% (w/w) in SEW48. In the CP-MAS spectrum of SEW36 (Fig. 2(D)) some carbohydrate signals are still visible in the anomeric region and the region containing the remaining ring C-atoms, although they have a much lower intensity than in SEW0. However, the most intense signals in SEW36 are identical to those in the spectrum of SEW48 (Fig. 2(E)), and thus represent signals from degradation products and microbes.

Characterization of ChSS and DASS.—Monosaccharide analysis of ChSS and DASS revealed an almost identical ratio between the

monosaccharides, suggesting that the polymers are identical (Table 4). However, enzymatic degradation experiments with both compounds revealed a better degradability of DASS compared with ChSS (Van Laar, unpublished results), indicating structural differences.

The CP-MAS spectra of ChSS (Fig. 3(A)) and DASS (Fig. 3(B)) were assigned (Tables 5 and 6, respectively) using the solid state NMR

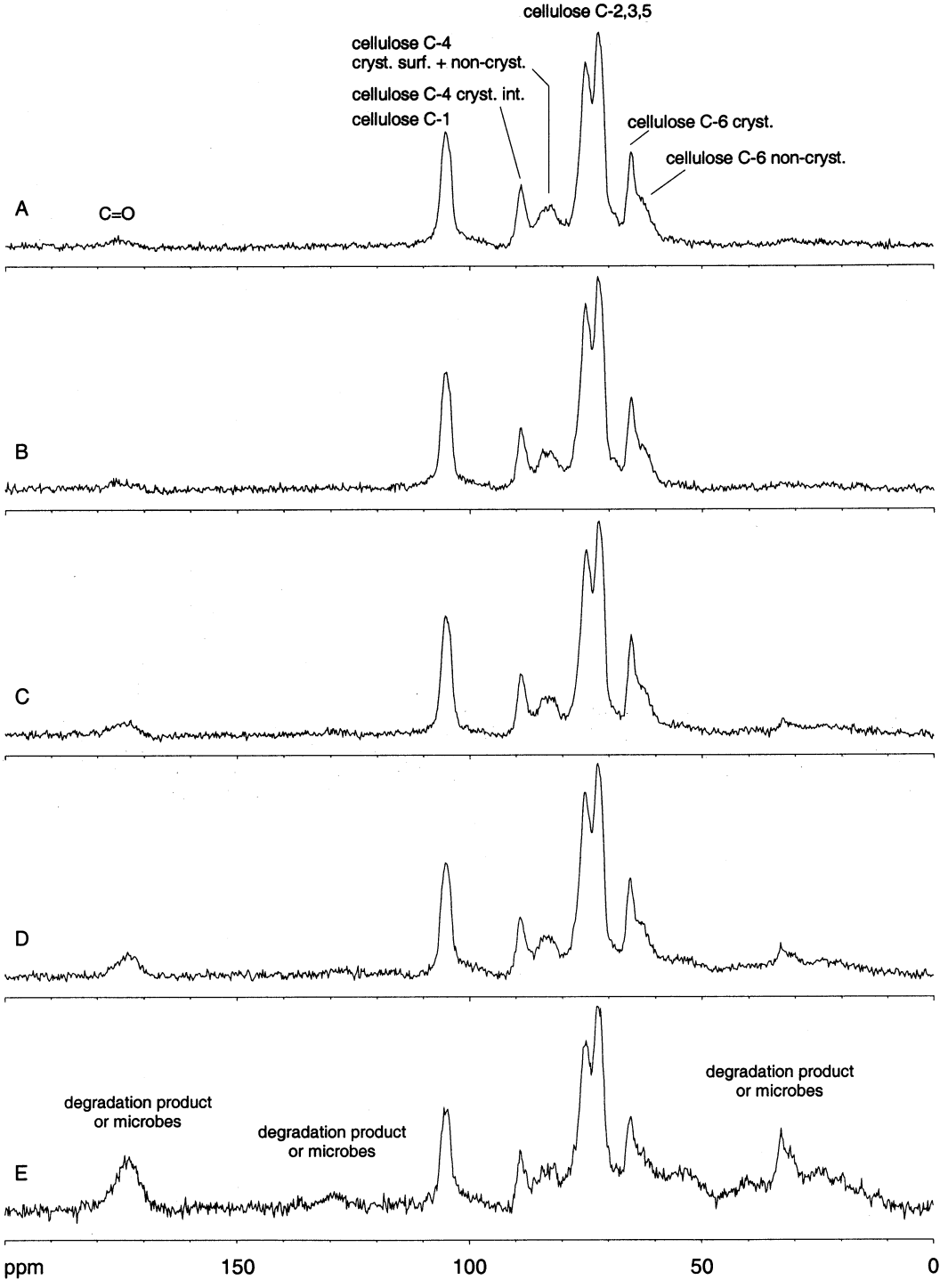

Fig. 1. CP-MAS spectra of soybean hull water unextractable solids incubated with sheep rumen fluid for (A) 0 h; (B) 12 h; (C) 24 h; (D) 36 h; and (E) 48 h. All spectra are recorded under the same experimental conditions and have been processed using an exponential multiplication (line broadening of 10) before Fourier transformation.

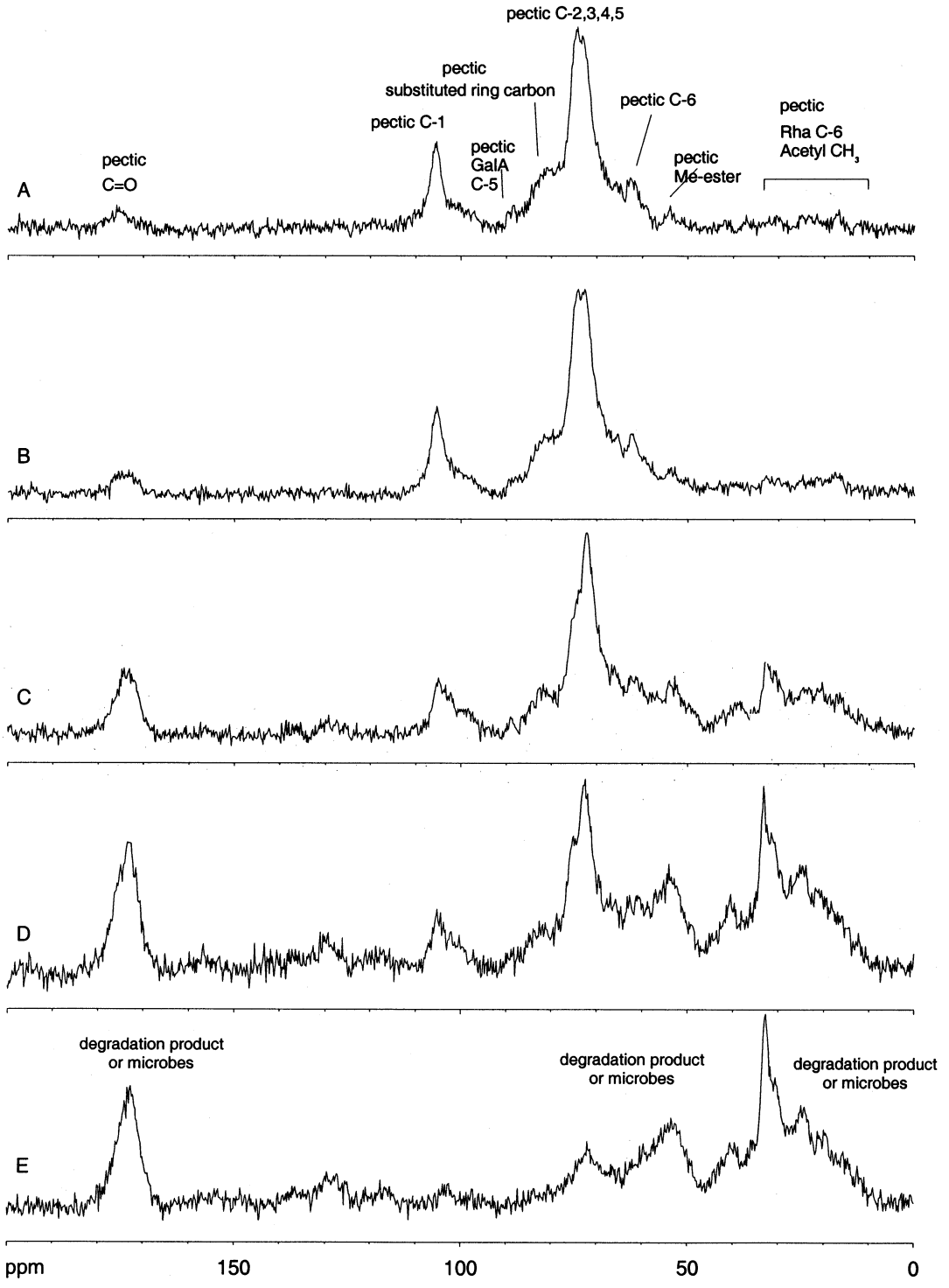

Fig. 2. CP-MAS spectra of soybean endosperm water unextractable solids incubated with sheep rumen fluid for (A) 0 h; (B) 12 h; (C) 24 h; (D) 36 h; and (E) 48 h. Each spectrum was recorded under the same experimental conditions and has been processed using an exponential multiplication (line broadening of 10) before Fourier transformation.

spectra of SEW and the solution state NMR spectra of ChSS, and compounds derived thereof [17]. CP-MAS spectra of both polymers showed comparable signals in the anomeric region and the region containing the remaining ring C-atoms. However, some differences in the other parts of the spectrum can be seen. The shift in the carboxyl signal (GalA C-6) from δ 172 (ChSS) to δ 174 (DASS) and the disappearance of the signal at δ 53 indi-

Table 4
Monosaccharide analysis of ChSS and DASS [a]

Compound	Ara	Fuc	Gal	GalA	Glc	Rha	Xyl
ChSS	24.2	3.0	37.0	20.8	1.3	4.4	9.3
DASS	24.4	3.4	34.2	23.7	0.7	4.2	9.4

[a] Expressed as mol%.

cate that the mild basic conditions used for the preparation of DASS saponified methyl esters in ChSS. The change in the carboxyl area and in the region δ 30–15 (CH_3 of acetyl groups and 6-deoxy sugars) suggest that acetyl groups have also been released. The saponification of the ester functions in DASS are probably responsible of the better degradation of DASS [26,27].

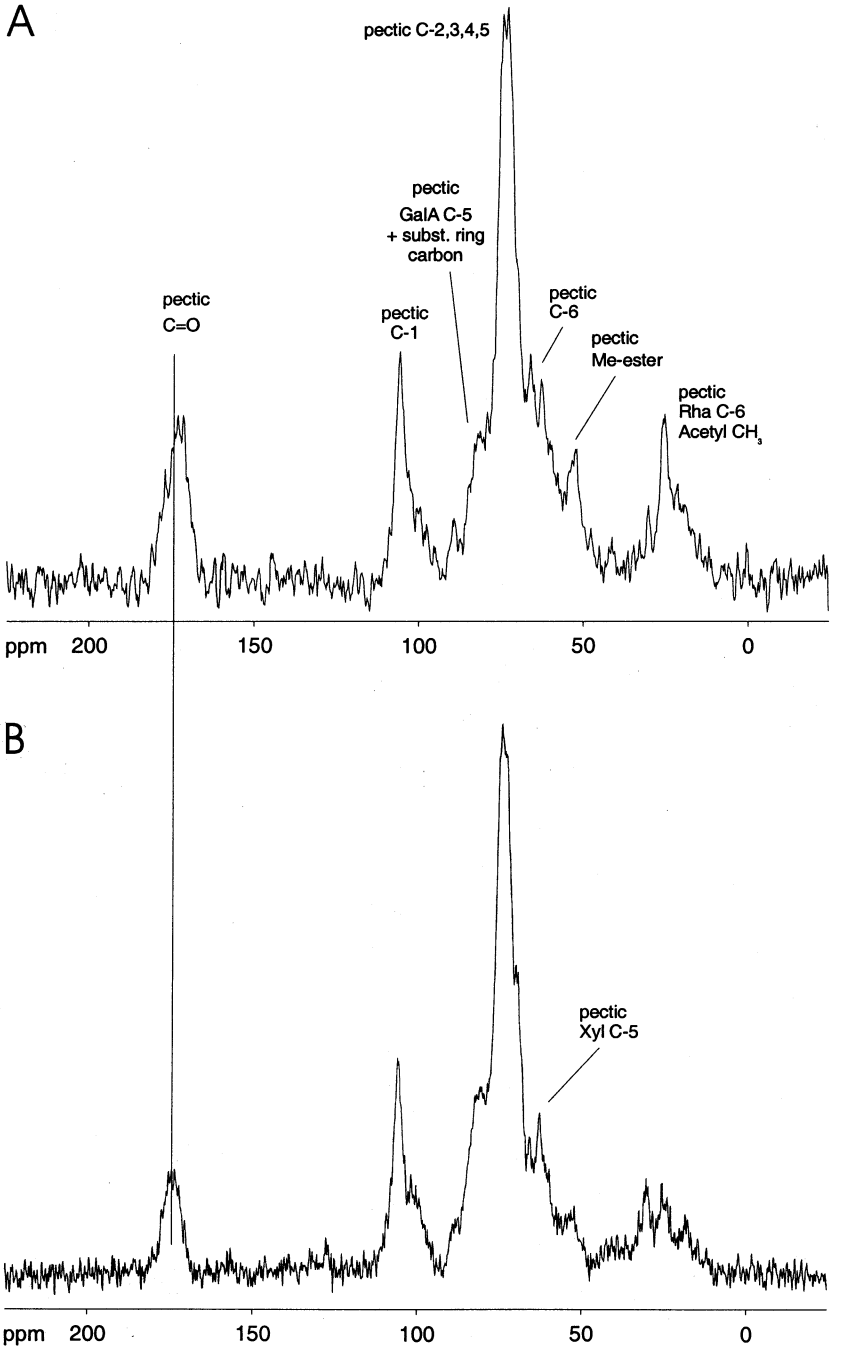

Fig. 3. CP-MAS spectrum of (A) ChSS and (B) DASS. Note the difference in chemical shift of the carbonyl signal (C=O) and the lower intensity of the signal at 53 ppm.

Table 5
Resonance assignments and fitting parameters [a] for the variable contact time experiment on ChSS [b]

Signal	Assignment [c]	$T_{CH\,A}$	$T_{1\rho\,A}$	$T_{CH\,B}$	$T_{1\rho\,B}$	A/B
172–156	C=O (carboxyl)	1.40	12.4			
104–91.5	C-1	1.39	6.8	0.06	6.7	0.92
91.5–84	C-5 GalA, subst. ring carbon	4.51	2.7	0.05	5.0	2.22
82–70	C-2,3,4,5	1.17	7.0	0.05	6.6	0.80
70–58	C-6	1.47	6.6	0.06	6.6	0.88
58–54.8	Xyl C-5	0.84	7.1	0.05	7.2	0.68
54.8–47.4	Me-ester	0.67	5.7	0.05	7.4	0.59
26–18.6	Rha C-6, acetyl CH_3	1.18	7.4	0.07	2.9	1.08

[a] The evaluation of the variable contact time experiments is based on the two-phase model (Eq. (2)), except for carbonyl functions, which have been evaluated with the mono-phase model (Eq. (1)). A/B represents the ratio between phase A and B.
[b] All time constants are in ms.
[c] Assignments of the different pectic signals are based on data in Ref. [17].

Table 6
Resonance assignments and fitting parameters [a] for the variable contact time experiment on DASS [b]

Signal	Assignment [c]	$T_{CH\,A}$	$T_{1\rho\,A}$	$T_{CH\,B}$	$T_{1\rho\,B}$	A/B
180–155	C=O (carboxyl)	0.37	12.3			
103.2–92.2	C-1	0.70	6.3	0.02	4.4	0.8
92.2–82.2	substituted ring carbon	1.30	4.0	<0.01	4.0	0.8
82.2–78.2	substituted ring carbon	0.90	3.8	<0.01	3.9	0.8
78.2–69.2	C-2,3,4,5	0.50	5.1	<0.01	4.6	0.8
69.2–54.7	C-6	0.78	7.3	0.01	3.8	0.8
54.7–46.7	Me-ester	0.39	8.3	0.01	4.6	0.7
33.7–18.2	Rha C-6, acetyl CH_3	0.74	3.9	0.02	6.7	0.7

[a] The evaluation of the variable contact time experiments is based on the two-phase model (Eq. (2)), except for carbonyl functions, which have been evaluated with the mono-phase model (Eq. (1)). A/B represents the ratio between phase A and B.
[b] All time constants are in ms.
[c] Assignments of the different pectic signals are based on data in Ref. [17].

Comparing mobility using a variable contact time CP-MAS experiment.—For each of the aforementioned compounds, 18–20 CP-MAS spectra were recorded with various contact times (0.05–20 ms). For each ^{13}C signal, the experimental intensity was evaluated as a function of the contact time. From these data, T_{CH} and $T_{1\rho}$ values were calculated using Eqs. (1) and (2). Least-squares fitting of the experimental data to Eqs. (1) and (2) revealed that the second model gave closer fits (Fig. 4). Therefore, the two-phase model was used for the analysis of different signals (Tables 1–3, 5 and 6). The ratio between the two phases is indicated with A/B. Carbonyl carbon signals were evaluated with the mono-phase model, as no hydrogen atom is linked to them.

Mobility of SHW 0 and SHW 48.—The presence in the CP-MAS spectrum of SHW48 of cellulose signals renders it possible to compare the mobility parameters of SHW0 with those of the partially degraded cellulose in SHW48 (Tables 1 and 2). The mobility of the C-1 through C-6 atoms in cellulose can be compared via their $T_{1\rho}$ values. The calculated values for $T_{1\rho}$ of different cellulose signals were in good agreement with those reported [22]. From the calculated values, as shown in Tables 1 and 2, it can be concluded that the mobility of the cellulose fibers in SHW remains unaltered during the degradation process. However, the relative amount of cellulose in the sample decreases, as follows from monosaccharide analyses and the signal-

to-noise ratios of the different signals in the CP-MAS spectra. These results can be explained by a layer-by-layer way of degradation of the long cellulose fibers [28]. The fitting results of the experimental data (Table 1) reveal that the magnetization intensity can be described with a slow and a fast phase (A and B, respectively). The time constant for the cross polarization of phase A ($T_{CH\,A}$) is quite invariable (0.4 ± 0.1 ms) for the different cellulose carbon atoms. The more mobile phase (B) has more variance in both $T_{1\rho}$ and T_{CH}. The calculated T_{CH} values are in good agreement with those reported in Ref. [24]. $T_{1\rho}$ values cannot be compared with those of Jarvis et al. [24] and Ha et al. [19], because they used a two-phase model with only one value for $T_{1\rho}$. Interestingly, the values for the slow phase (A) are in good agreement with those reported in Ref. [19]. The degradation products or microbes in SHW48 have lower $T_{1\rho}$ values than the cellulose signals, indicative of a higher mobility of these products.

Mobility of SEW 0, SEW 48, ChSS, and DASS.—The CP-MAS spectrum of SEW48 shows that the starting material (SEW0) has disappeared after 48 h of incubation, as is clear from the intensity of the signal in the anomeric region. As the degradation products in SEW48 are probably identical to the ones in SHW48, no variable contact time experiments were recorded for this material.

The proton $T_{1\rho}$ values of SEW, ChSS, and DASS are shorter than those of SHW (cellulose). This corresponds to the cellular functions of the different polymers. Cellulose is the load-bearing component. It occurs as long very rigid fibers in the plant cell wall. SEW, ChSS and DASS all predominantly contain pectins. These acidic polysaccharides account for example for the cell wall porosity [29]. Therefore, pectins should be more flexible than cellulose (SHW), which is apparent from their lower proton $T_{1\rho}$ values.

The pectins in SEW and ChSS (Tables 3 and 5, respectively) are partly present in the form of methyl-esterified carboxyl functions, and contain O-acetyl groups, in contrast to DASS (Table 6). This is reflected by the value for T_{CH}, that is lower in DASS ($T_{CH} = 0.37$ ms) than in ChSS ($T_{CH} = 1.40$ ms) or SEW ($T_{CH} = 1.11$ ms).

Finally, a 2D $^{1}H-^{13}C$ wideline separation (WISE) NMR spectrum of SEW0 was recorded. In this experiment, the ^{1}H spectral patterns associated with each of the well-resolved ^{13}C chemical shifts are displayed. Since ^{1}H spectral line widths reflect the size of the homonuclear dipolar coupling, the more rigid segments will exhibit wider lines. Structural information can be obtained from the ^{13}C chemical shifts [30,31]. The ^{1}H 1D spectrum is composed of two lineshapes (linewidth 45 and 2.2 kHz) in the non-spinning case, whereas the

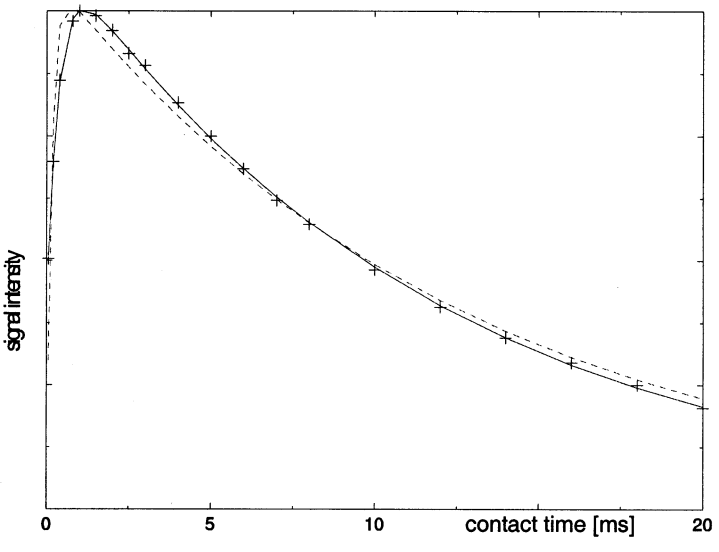

Fig. 4. Experimental signal intensity (+) of the SHW anomeric signal (δ 109–102.5) evaluated as a function of the contact time with the mono-phase model, Eq. (1) (---) and the two-phase model, Eq. (2) (—).

spinning spectrum (spinning frequency 9 kHz) consists of one sharp signal (linewidth 0.8 kHz). Each ^{13}C signal shows the same ^{1}H spectral pattern (linewidth 12 kHz), by consequence carbon atoms of this polymer have a similar rigidity.

4. Conclusions

CP-MAS NMR analysis of the polymers showed the possibilities of this technique in characterizing various plant cell-wall materials, such as cellulose and pectins.

Information about the rate of the degradation can be obtained from the relationship between the signal-to-noise ratio of carbohydrate signals in the CP-MAS NMR spectra and the incubation time. The difference in enzymatic fermentability between ChSS and DASS can be explained by the degree of methyl-esterification, which is lower in DASS. Furthermore, the proton $T_{1\rho}$ values suggest that cellulose fibers are degraded layer-by-layer by the enzymes present in the sheep rumen fluid. The higher mobility of SEW compared with SHW can cause a better accessibility of this polymer towards enzymes, which explains the faster degradation of SEW.

5. Experimental

Materials.—Full fat Argentinean soybeans were manually separated into hulls and endosperm. From both materials, polysaccharide fractions were isolated and starch was removed as described [15,18], yielding SEW (soy endosperm water unextractable solids) and SHW (soy hull water unextractable solids). Water unextractable solids (WUS) represents the carbohydrate fraction of the starting material, free of proteins and starch. WUS of the complete soybean was extracted with 1,2-diaminocyclohexane-*N*,*N*,*N*′,*N*′-tetra-acetic acid (CDTA) to give a chelating agent soluble solids fraction (ChSS), which yielded after extraction with 0.05 M NaOH, a dilute alkali soluble solids (DASS) fraction [15]. For the in vitro degradation of SEW and SHW, sheep rumen fluid was used as inoculum, as described [18].

NMR spectroscopy.—NMR samples were lyophilized from water solns before measurement. ^{13}C CP-MAS NMR spectra were recorded at ambient temperature on a Bruker DMX 300 spectrometer (NSR center, University of Nijmegen), operating at 300 and 75 MHz for ^{1}H and ^{13}C, respectively. Samples were packed into 3-mm rotors and spun at 9.0 kHz at the magic angle (54.7°) with respect to the static magnetic field. A 90° pulse length of 3.0 μs was used for ^{1}H. Chemical shifts for ^{13}C are expressed in ppm relative to external adamantane (CH_2 at δ 38.3). The ^{13}C spectra and proton $T_{1\rho}$ values were obtained with a CP pulse sequence using a ramp shape on carbons to enhance sensitivity [32,33]. Contact times for proton $T_{1\rho}$ experiments varied from 50 μs to 20 ms (DASS 16 ms). In ^{13}C CP-MAS experiments, the contact time was set to 2 ms and the recycle delay was set to 4 s. CP-MAS spectra of SHW0, -12, -24, -36, -48 and SEW0, -12, -24, -36, -48 were recorded under the same experimental conditions with an equal number of scans.

Experimental data of the variable contact time experiments were fitted using XMGR 4.1.2 (copyright © 1991–95 Paul J. Turner, Portland, or copyright © 1996–98 ACE/gr Development Team).

Acknowledgements

The authors would like to thank Ms G.H. Nachtegaal (NSR Center, Department of Physical Chemistry, University of Nijmegen, The Netherlands) and Dr F. Ruhnau (Bijvoet Center, Department of Bio-Organic Chemistry, Utrecht University, The Netherlands) for their assistance with the NMR experiments. These investigations were supported by the Dutch Technology Foundation (NWO/STW), Gist-brocades, The Product Board for Feeding Stuffs (VVR). The NMR spectra were obtained at the NSR Center (University of Nijmegen, The Netherlands).

References

[1] R.W. Bailey, J.A. Monro, S.E. Pickmere, A. Chesson, in H. Veenman, B.V. Zonen (Eds.), *Carbohydrate Research in Plants and Animals*, Wageningen, 1976, pp. 1–16.

[2] M.S. Kerley, G.C. Fahey Jr., J.M. Gould, E.L. Iannotti, *Food Microstruct.*, 7 (1988) 59–65.
[3] M. Morita, *Agric. Biol. Chem.*, 29 (1965) 564–573.
[4] M. Morita, *Agric. Biol. Chem.*, 29 (1965) 626–630.
[5] M. Morita, M. Okuhara, T. Kikuchi, Y. Sakurai, *Agric. Biol. Chem.*, 31 (1967) 314–318.
[6] G.O. Aspinall, J.N.C. Whyte, *J. Chem. Soc.*, (1964) 5058–5063.
[7] G.O. Aspinall, K. Hunt, I.M. Morrison, *J. Chem. Soc.*, (1966) 1945–1949.
[8] G.O. Aspinall, R. Begbie, A. Hamilton, J.N.C. Whyte, *J. Chem. Soc.*, (1967) 1065–1070.
[9] G.O. Aspinall, I.W. Cottrell, S.V. Egan, I.M. Morrison, J.N.C. Whyte, *J. Chem. Soc.*, (1967) 1071–1080.
[10] G.O. Aspinall, K. Hunt, I.M. Morrison, *J. Chem. Soc.*, (1967) 1080–1086.
[11] G.O. Aspinall, I.W. Cottrell, *Can. J. Chem.*, 49 (1971) 1019–1022.
[12] J.M. Labavitch, L.E. Freeman, P. Albersheim, *J. Biol. Chem.*, 251 (1976) 5904–5910.
[13] A. Bacic, P.J. Harris, B.A. Stone, in J. Preiss (Ed.), *The Biochemistry of Plants a Comprehensive Treatise*, Vol. 14 *Carbohydrates*, Academic Press, San Diego, 1988, pp. 297–371.
[14] M. O'Neill, P. Albersheim, A.G. Darvill, in P.M. Dey (Ed.), *Methods in Plant Biochemistry*, Vol. 2, Academic Press, London, 1999, pp. 415–441.
[15] M.M.H. Huisman, H.A. Schols, A.G.J. Voragen, *Carbohydr. Polym.*, 37 (1998) 87–95.
[16] M.M.H. Huisman, H.A. Schols, A.G.J. Voragen, *Carbohydr. Polym.*, 38 (1999) 299–307.
[17] M.M.H. Huisman, C.T.M. Fransen, J.P. Kamerling, J.F.G. Vliegenthart, H.A. Schols, A.G.J. Voragen, *Biopolymers* (2000) in press.
[18] H. van Laar, S. Tamminga, B.A. Williams, M.W.A. Verstegen, F.M. Engels, *Anim. Feed Sci. Technol.*, 79 (1999) 179–193.
[19] M.-A. Ha, B.W. Evans, M.C. Jarvis, D.C. Apperley, A.M. Kenwright, *Carbohydr. Res.*, 288 (1996) 15–23.
[20] L.B. Alemany, D.M. Grant, R.J. Pugnire, T.D. Alger, K.W. Zilm, *J. Am. Chem. Soc.*, 105 (1983) 2133–2141.
[21] M. Mehring, *High Resolution NMR Spectroscopy in Solids*, Springer, Berlin, 1976.
[22] R.H. Newman, J.A. Hemmingson, *Cellulose*, 2 (1994) 95–100.
[23] R.H. Newman, M.-A. Ha, L.D. Melton, *J. Agric. Food Chem.*, 42 (1994) 1402–1406.
[24] M.C. Jarvis, K.M. Fenwick, D.C. Apperley, *Carbohydr. Res.*, 288 (1996) 1–14.
[25] H. van Laar, Thesis, Wageningen University, The Netherlands, 2000, pp. 51–68.
[26] E.J. Morris, J.S.D. Bacon, *J. Agric. Sci. Camb.*, 89 (1977) 327–340.
[27] A. Chesson, *J. Sci. Food Agric.*, 32 (1981) 745–758.
[28] A. Chesson, in H.G. Jung, D.R. Buxton, R.D. Hatfield, J. Ralph (Eds.), *Forage Cell Wall Structure and Digestibility*, American Society of Agronomy Inc., Crop Science Society of America Inc., Soil Science Society of America Inc., Madison, pp. 347–374.
[29] M.C. McCann, K. Roberts, in J. Visser, A.G.J. Voragen (Eds.), *Progress in Biotechnology*, Vol. 14, *Pectins and Pectinases*, Elsevier, Amsterdam, 1996, pp. 91–107.
[30] K. Schmidt-Rohr, J. Clauss, H.W. Spiess, *Macromolecules*, 25 (1995) 3273–3277.
[31] B. Yan, R.E. Stark, *Macromolecules*, 31 (1998) 2600–2605.
[32] G. Metz, X.L. Wu, S.O. Smith, *J. Magn. Reson. Ser. A*, 110 (1994) 219–227.
[33] S. Hediger, B.H. Meier, R.R. Ernst, *Chem. Phys. Lett.*, 213 (1993) 627–635.
[34] W.L. Earl, D.L. VanderHart, *Macromolecules*, 14 (1981) 570–574.